



Design and fabrication of a CH/Al dual-layer perturbation target for hydrodynamic instability experiments in ICF



Jun Tang^a, Zhiyong Xie^b, Ai Du^a, Junjian Ye^b, Zhihua Zhang^a, Jun Shen^a, Bin Zhou^{a,*}

^a Shanghai Key Laboratory of Special Artificial Microstructure Materials and Technology, School of Physics Science and Engineering, Tongji University, Shanghai 200092, China

^b Shanghai Institute of Laser Plasma, Shanghai 201800, China

HIGHLIGHTS

- Sinusoidal perturbed Al foil was prepared by single-point diamond turning.
- Perturbed Al foil was measured by surface profiler and white light interferometer.
- Perturbed Al foil and CH layer adhered with each other via a hot-press process.
- Parameters and cross-section of the CH–Al perturbation target was characterized.

ARTICLE INFO

Article history:

Received 12 November 2013

Received in revised form 5 April 2014

Accepted 5 April 2014

Available online 2 May 2014

Keywords:

Hydrodynamic instability

Dual-layer perturbation target

Single-point diamond turning technology

Inertial confinement fusion

ABSTRACT

A polystyrene (CH)/aluminum (Al) dual-layer perturbation target for hydrodynamic instability experiments in inertial confinement fusion (ICF) was designed and fabricated. The target was composed of a perturbed 40 μm Al foil and a CH layer. The detailed fabrication method consisted of four steps. The 40 μm Al foil was first prepared by roll and polish process; the perturbation patterns were then introduced on the surface of the Al foil by the single-point diamond turning (SPDT) technology; the CH layer was prepared via a simple method which called spin-coating process; finally, the CH layer was directly coated on the perturbation surface of Al foil by a hot-press process to avoid the use of a sticker and to eliminate the gaps between the CH layer and the Al foil. The parameters of the target, such as the perturbation wavelength (T) and perturbation amplitude (A), were characterized by a QC-5000 tool microscope, an alpha-step 500 surface profiler and a NT1100 white light interferometer. The results showed that T and A of the target were about 52 μm and 7.34 μm , respectively. Thickness of the Al foil (H_1), thickness of the CH layer (H_2), and cross-section of the dual-layer target were characterized by a QC-5000 tool microscope and a scanning electron microscope (SEM). H_1 and H_2 were about 40 μm and 15 μm , respectively, the cross-sectional photographs of the target showed that the CH layer and the Al foil adhered perfectly with each other.

© 2014 Elsevier B.V. All rights reserved.

1. Introduction

In inertial confinement fusion (ICF) experiments, when the ignition target capsule is irradiated by a high-intensity laser facility, such as NIF, Nova, Omega and LMJ, the hydrodynamic instability occurred for the spatial distribution uniformity of laser intensity and the roughness of target capsule [1,2]. Understanding and controlling the growth of hydrodynamics instability can increase

the feasibility of ignition experiments strongly. So research of the hydrodynamic instability has been focus for years [3–6]. In general, an ignition capsule usually consists of several layers with different density, such as low-Z ablator material, foam, deuterium–tritium (DT) ice, DT gas and so on [7]. When the capsule is driven by high intensity laser for direct-driven or by X-ray for indirect-driven, the outer layer is ablated and the instability, seeded by target imperfection and nonuniform irradiation, can grow via Rayleigh–Taylor (RT) instability in the ablate and centripetal compress process [8,9]. In recent years, many different kinds of experiments and targets had been designed and fabricated to simulate and investigate the growth of RT instability. Such as single layer targets [10–12], dual-layer targets [13–15], multilayer targets [16–19] and so on. The

* Corresponding author at: No. 1239 Siping Road, Yangpu District, 200092 Shanghai, China. Tel.: +86 21 6598 2762; fax: +86 21 6598 6071.

E-mail addresses: zhoubin863@tongji.edu.cn, charmantang@126.com (B. Zhou).

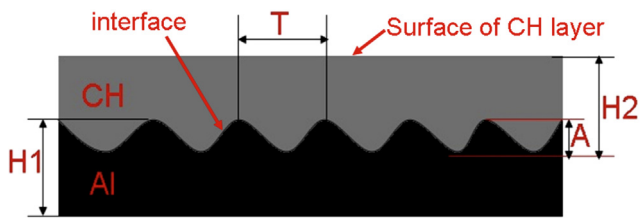


Fig. 1. Schematic of the CH/Al dual-layer perturbation target.

dual-layer targets, for the Atwood number $Ad = (\rho_2 - \rho_1)/(\rho_2 + \rho_1)$ can be changed easily by changing the materials of the component layer, they are widely used in simulating the growth of RT instability. In this article, a polystyrene (CH)/aluminum (Al) dual-layer perturbation target was designed and fabricated to simulate the growth of RT instability in ICF. Sinusoidal perturbation patterns were introduced on the surface of Al foil by the single-point diamond turning (SPDT) technology. The CH layer was directly coated on the perturbation surface of the Al foil by a hot-press process. The perturbation patterns were used as the seed for RT instability growth when the ablator shock wave traveled through the interface of the CH layer and the Al foil. Target parameters, such as the perturbation wavelength (T), perturbation amplitude (A), were characterized by a QC-5000 tool microscope, an alpha-step 500 surface profiler and a NT1100 white light interferometer. Thickness of the Al foil ($H1$), thickness of the CH layer ($H2$), and cross-section of the dual-layer target were characterized by a QC-5000 tool microscope and a scanning electron microscope (SEM).

2. Experimental

2.1. Design of the CH/Al dual-layer perturbation target

The CH/Al dual-layer perturbation target was designed to research the RT instability in ICF. The CH polymer, a low- Z material composed of C and H elements, with a density of 1.03 g/cm^3 , exhibits high energy deposition and good machinability, chosen as the preferred outer ablator material [20,21]. The aluminum, a metal with a density of 2.7 g/cm^3 and good ductility, chosen as the tamper of the dual-layer target to fabricate an unstable target ($Ad \sim 0.45$) for the RT instability experiments in ICF. As the seed for RT instability growth, the perturbation patterns were introduced on the surface of the Al foil by the SPDT technology, then the CH layer was directly coated on the perturbation surface of Al foil by a hot-press process to avoid the use of a sticker and to eliminate the gaps between the CH layer and the Al foil. Fig. 1 shows the schematic of the CH/Al dual-layer perturbation target.

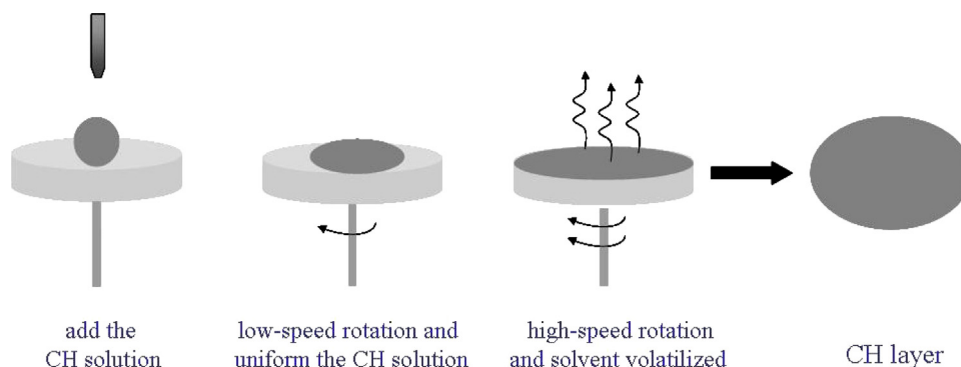


Fig. 2. Schematic of the spin-coating process.

2.2. Pre-treatment of the Al foil before introduce the perturbation patterns

The Al foil prepared by roll process with large surface roughness, so the surface of Al foil needs polish first to reduce the surface roughness before the perturbation patterns introduced on it. The polish process was described as follows. The rolled $40 \mu\text{m}$ Al foil was flattened on the quartz glass, grinded by the polishing paste and a polisher. Then ultrasonic cleaned by acetone, ethyl alcohol and deionized water in sequence to remove the residual impurities. Finally, the cleaned Al foil blow-dried by nitrogen and reserved for introduce the perturbation patterns by SPDT technology.

2.3. Introduce the perturbation on the surface of Al foil by the SPDT technology

Perturbation patterns were introduced on the surface of Al foil by the SPDT technology [22]. The Al foil was gripped via a vacuum negative pressure, and cut by a natural diamond cutter. The whole lathe and spindle use the air-flotation method to reduce the impact of external vibration. Numerical control resolution of the lathe was 1 nm ; precision of second grip was controlled under $1 \mu\text{m}$. Curvature radius of the diamond cutter was $2 \mu\text{m}$. The Al foil was cooled by spray cooling during the cut process, the cuttings were drawn away by a air pump to avoid the cuttings not only damage the processed surface of the Al foil, but also pollute the machining environment. The machining environment was 20°C , humidity 40% and ultraclean class of 10 000.

2.4. Preparation of the CH layer by spin-coating process

The CH layer was prepared by a spin-coating process. Solid CH (purity: 99.9%) was dissolved in chloroform and stirred with a magnetic bar for 4 h, then vibrated in an ultrasonic bath for 2 h. After this, the CH solution filtered with a qualitative filter paper to obtain a transparent, uniform CH solution. In order to obtain the CH solution with appropriate concentration for spin-coating, the solution was continuing stirred with a magnetic bar to make the solvent chloroform volatilized gradually. For CH layer preparation, the CH solution was dropped upon a circular, smooth quartz glass with a diameter of 35 mm and which was fixed by the adsorption devices of the spin coater. First, the glass was spinning with a low-speed about 100 rpm for 3 s to uniform the CH solution on the glass. And then, the spinning speed of the glass was quickly accelerated to about 2500 rpm and kept for 30 s to make the solvent chloroform volatilized and form a CH film on the glass. Finally, took off the CH film from the quartz glass, the CH layer was obtained. Fig. 2 shows the schematic of this spin-coating process. Thickness of the

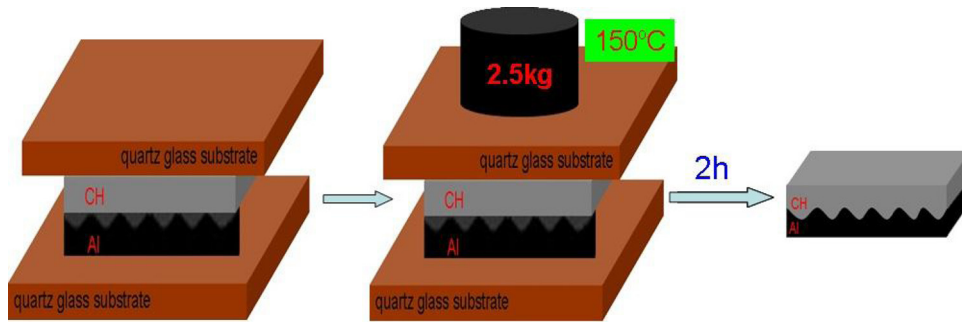


Fig. 3. Schematic of the hot-press process.

CH layer was controllable via adjust the concentration of the CH solution and the spinning speed of the quartz glass.

2.5. Coated the CH layer onto the perturbed Al foil by hot-press process

For dual-layer target formation, the CH layer and the perturbed Al foil need to adhered with each other. In this article, the CH layer was coated on the perturbed Al foil directly by a hot-press process. First, the perturbed Al foil was flattened on the quartz glass substrate with the perturbation surface up, the CH layer coated on the Al foil and another quartz glass substrate covered the CH layer. Then the whole four parts put into a muffle furnace at 150 °C and a 2.5 kg weight pressed on them for 2 h. As the CH layer been heated and pressed, the CH layer soften, adhered with the Al foil and filled the gaps between the CH layer and the valley of the perturbed Al foil.

Finally, the four parts was cooled naturally to room temperature, and then the CH/Al dual-layer perturbation target was obtained by cut manually. Fig. 3 shows the schematic of the hot-press process.

2.6. Measurement of the target and target parameters

The parameters of the target, such as the perturbation wavelength (T), perturbation amplitude (A), were characterized by a QC-5000 tool microscope (Metronics QC-5000, resolution: ± 0.001 mm), an alpha-step 500 surface profiler (Tencor Corporation, Alpha-step500) and a NT1100 white light interferometer. Thickness of the Al foil ($H1$), thickness of the CH layer ($H2$), and cross-section of the dual-layer target were characterized by QC-5000 tool microscope and scanning electron microscope (SEM, Philips-XL30FEG) as well. Surface roughness of the CH layer

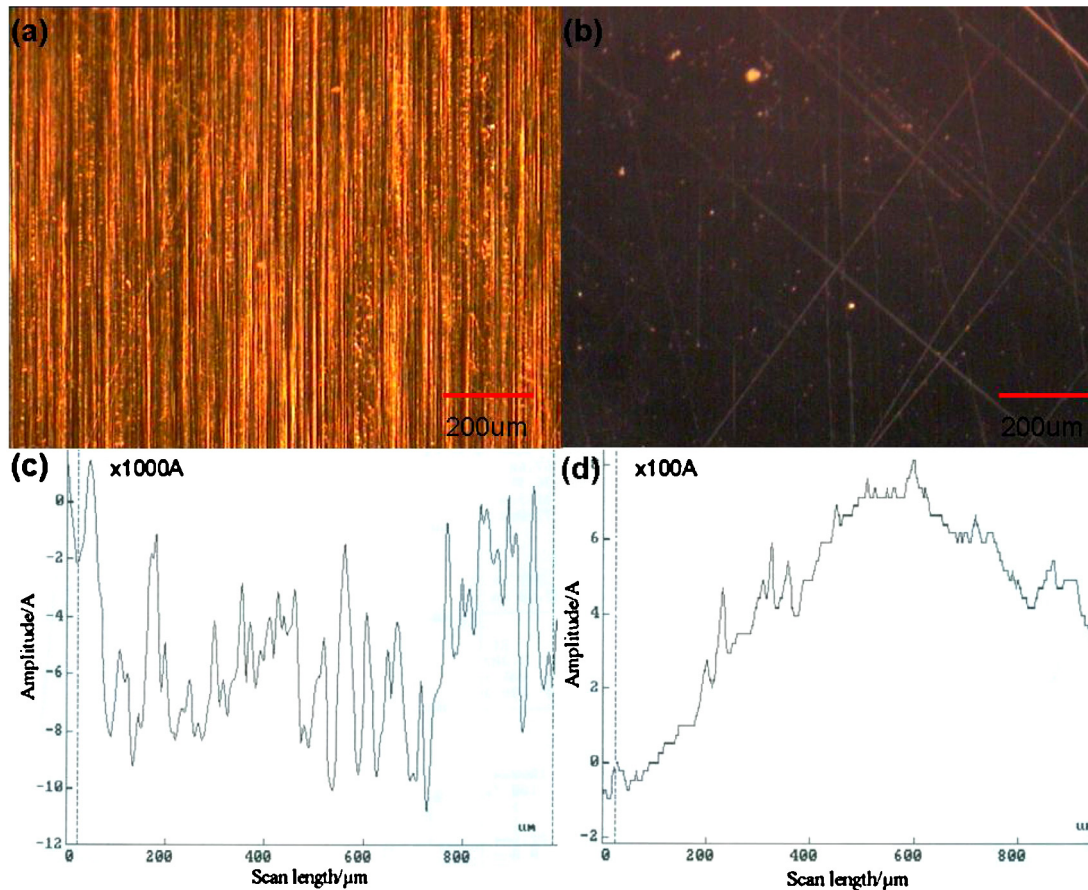


Fig. 4. Surface and surface roughness of the Al foil: (a) and (c) were before polished; (b) and (d) were after polished.

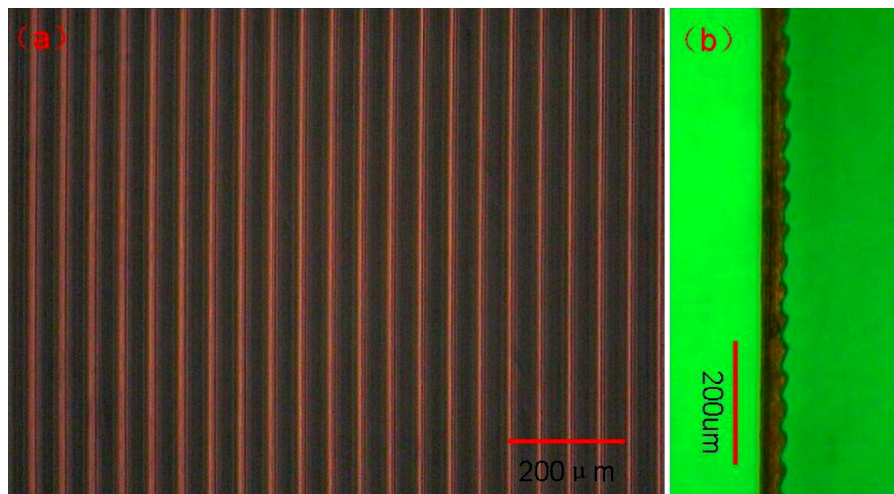


Fig. 5. Enlarged view of the perturbed Al foil: (a) surface of Al foil and (b) cross-section of Al foil.

surface was also measured by alpha-step 500 surface profiler (Tencor Corporation, Alpha-step500).

3. Results and discussion

3.1. Polishing treatment of the Al foil

Fig. 4(a) and (b) shows the surface of the Al foil before and after polish, respectively. In Fig. 4(a) the surface of the Al foil was rough, while in Fig. 4(b), the surface was smoother. A smooth surface of the Al foil was necessary to introduce the perturbation patterns. Fig. 4(c) and (d) shows the quantitative surface roughness of the Al foil before and after polish, respectively, scanning length of them were both 1 mm. In Fig. 4(c), the maximum fluctuation was over $1 \mu\text{m}$, the surface average roughness (R_a) and the root mean square roughness (R_q) were 212.72 nm and 261.38 nm . While in Fig. 4(d), the maximum fluctuation was under $0.1 \mu\text{m}$; R_a and R_q were 16.8 nm and 19.5 nm . Compared these two results, it indicated that the polish process reduced the surface roughness substantially.

3.2. Perturbation patterns on the surface of the Al foil

After been polished, the perturbation patterns were introduced on the surface of Al foil by the SPDT technology. Fig. 5 shows the enlarged view of the Al foil after been perturbed, (a) was the surface of the perturbed Al foil which shows a uniform T about $50 \mu\text{m}$, and (b) was the cross-section of the perturbed Al foil which shows not only a uniform T about $50 \mu\text{m}$ but also a uniform A about $8 \mu\text{m}$. In the turning process, as the scale of perturbation patterns was small, a sharp edge cutter with curvature radius of $2 \mu\text{m}$ was chosen to cut the Al foil. Under this condition, the perturbation patterns with T/A of 5–10 could obtain.

In order to get precise T and A of the perturbation patterns, a surface profiler was used to characterize the perturbed Al foil. The Al foil was flattened on the test platform of the profiler, the probe of the profiler scanning over the perturbation surface of the Al foil. The scanning length and scanning speed were $450 \mu\text{m}$ and $50 \mu\text{m s}^{-1}$, respectively, and the results were shown in Fig. 6. In this figure, uniform T and A of the perturbation patterns were shown clearly, and could read precisely as $52 \mu\text{m}$ and $7.34 \mu\text{m}$, respectively. The perturbation patterns were very similar to the sinusoidal fluctuate, which meet the requirements of the hydrodynamic instability experiments in ICF well.

In order to observe three-dimensional image of the perturbation patterns on the surface of the Al foil more intuitively, a white

light interferometer was used to measure the perturbation surface of the Al foil. The perturbed Al foil was flattened on the test platform of the white light interferometer, and enlarged $50\times$. The three-dimensional image of the perturbation patterns was shown in Fig. 7. In this figure, A and T were uniform as well, and were $7.97 \mu\text{m}$ and $52 \mu\text{m}$, respectively. The result of T was agreed with the result which was measured by the surface profiler, while the result of A was some deviation to the result measured by the surface profiler. As the surface profiler was a contact and more precise measuring method, and the white light interferometer have some deviation especially when the magnification was large, the result measured by the surface profiler was considered to be the credible one, so the perturbation amplitude A was $7.34 \mu\text{m}$. What's more, this little deviation had no great influence for observing the three-dimensional image of the perturbation patterns. The perturbation patterns were very close to the sinusoidal fluctuate.

3.3. Adjust the thickness of the CH layer

Thickness of the CH layer was controllable via adjusting the concentration of the CH solution and the spinning speed of the quartz glass. Based on large amounts of experimentations, experiential relationship of the thickness of the CH layer and the

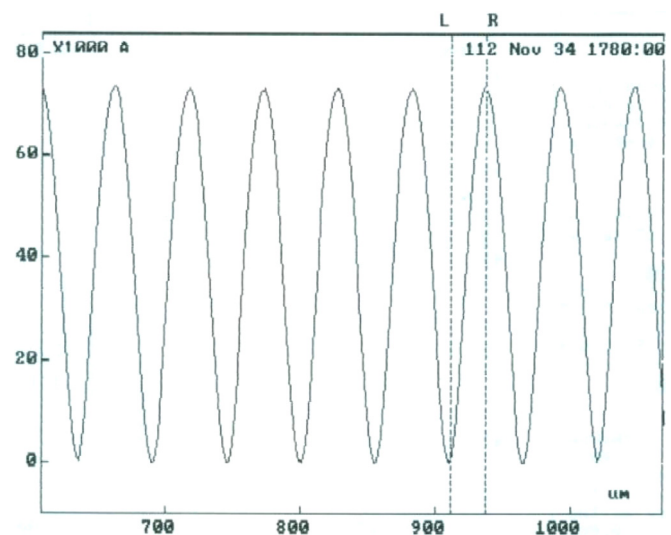


Fig. 6. Perturbation patterns on the surface of the Al foil.

Table 1
Thickness of the CH layer and the concentration of the CH solution, the spinning speed of the quartz glass.

Concentration of the CH solution W%	Thickness of the CH layer (μm) at different spin speed (rpm)				
	1000	1500	2000	2500	3000
8	12	10	8	/	/
12	20	16	12	9	6
16	33	22	18	14	9
20	/	27	24	20	12
24	/	/	30	24	16

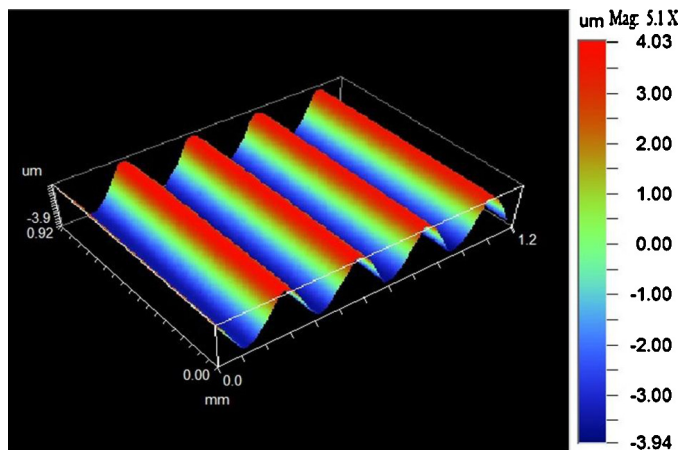


Fig. 7. Three-dimensional image of the perturbation patterns on the surface of the Al foil.

concentration of the CH solution, the spinning speed of the quartz glass was shown in Table 1. The spin-coating process was the same as Section 2.4, 3 s for 100 rpm and 30 s for each high spinning speed listed in Table 1. The results indicated that the concentration of the CH solution higher or the spinning speed of the quartz glass lower, the CH layer obtained thicker. Uniform (in 1 mm length, the maximum fluctuation was under $0.5 \mu\text{m}$, the surface average roughness (R_a) and root mean square roughness (R_q) both under $0.15 \mu\text{m}$) CH layer could obtain was about 8–33 μm .

3.4. Parameters of the CH/Al dual-layer perturbation target

The CH layer was coated on the perturbed Al foil directly by a hot-press process. Fig. 8 shows the picture of CH/Al dual-layer perturbation target, (a) was the face-on view. As the CH layer was transparent, the perturbation patterns on the surface of the Al foil can be seen clearly, this picture almost has no difference with Fig. 5(a). Fig. 8(b)–(d) shows the cross-section view of the CH/Al dual-layer perturbation target; (b) shows the cross-section image measured by the QC-5000 tool microscope. In this picture, the CH layer and the perturbed Al foil adhered with each other,

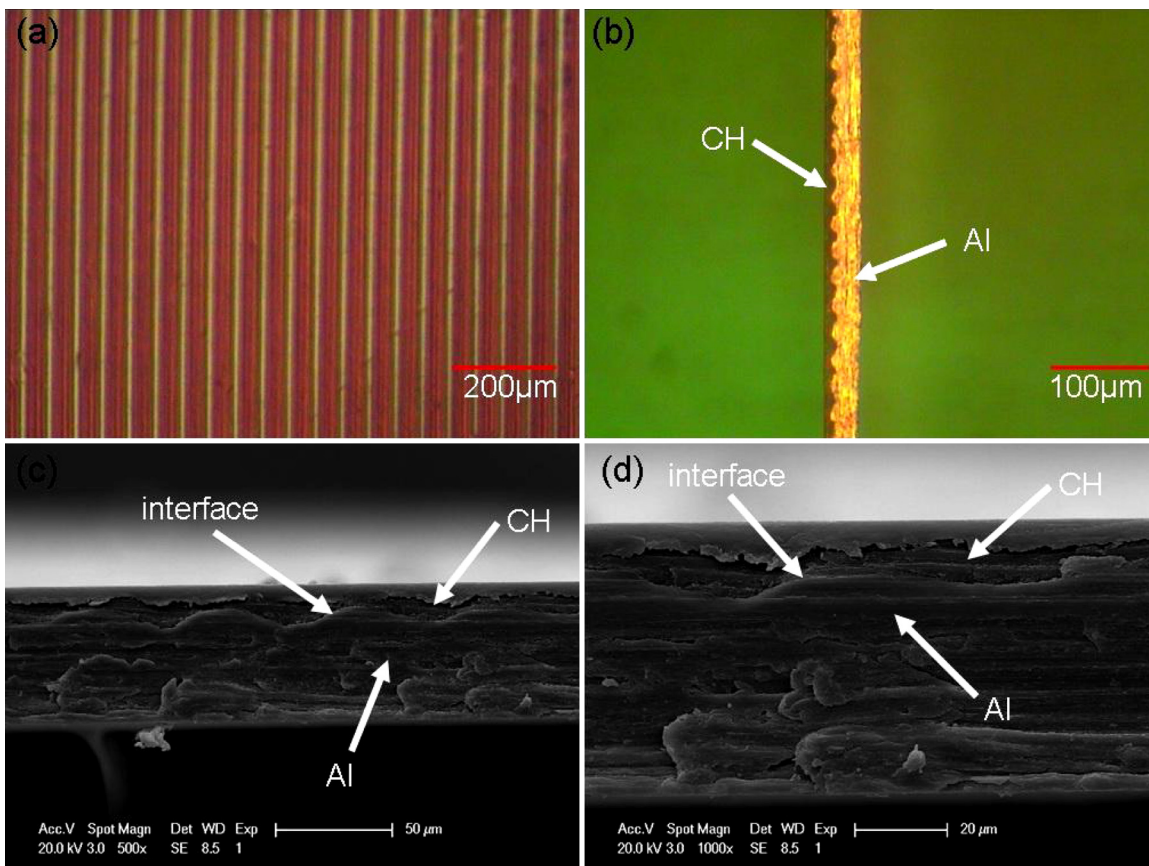


Fig. 8. CH/Al dual-layer perturbation target: (a) face-on view and (b)–(d) cross-section.

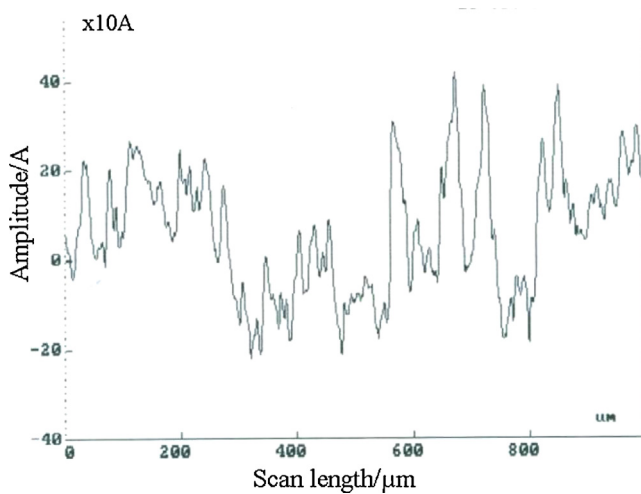


Fig. 9. Surface roughness of the CH layer.

the perturbation patterns were introduced into the interface between the CH layer and the Al foil as the seed for the growth of RT instability successfully. More detailed cross-section images measured by SEM were shown in Fig. 8(c) and (d). These two pictures indicated that the interface between the two layers has no gaps, these two layers combined well, and the perturbation patterns introduced into the interface between these two layers successfully. H1 and H2 were $40\ \mu\text{m}$ and $15\ \mu\text{m}$, respectively.

3.5. Surface roughness of the CH layer surface

Surface roughness of the CH layer surface has important influence on the hydrodynamic instability experiments in ICF, so a surface profiler was used to characterize the surface roughness of the CH layer. The characterizing method was the same to which described in Section 3.2. The scanning length and scanning speed were $1000\ \mu\text{m}$ and $100\ \mu\text{m}\ \text{s}^{-1}$, respectively. The results were shown in Fig. 9, the surface average roughness (R_a) and root mean square roughness (R_q) of the CH layer surface were measured to be $11.47\ \text{nm}$ and $13.62\ \text{nm}$, respectively, far less than the wavelength of the driven laser ($530\ \text{nm}$). Which revealed that the CH layer surface of the dual-layer target have good surface smoothness, meet the requirements of the hydrodynamic instability experiments well.

3.6. Influence of the hot-press process to the perturbation of the Al foil

In the hot-press process, the Al foil was heated to 150°C and pressed by $2.5\ \text{kg}$ weight, the amplitude and wavelength of the perturbation patterns might have changed after been hot-pressed. In order to evaluate the effect, that hot-pressing the CH onto the perturbed Al foil has on the amplitude and wavelength of the perturbation, the CH/Al dual-layer perturbation target was cleaned by chloroform to remove the CH layer, the amplitude and wavelength of the perturbation were measured by a surface profiler again. The measuring method was the same as Section 3.2 and the results were shown in Fig. 10. In this figure, uniform T and A of the perturbation were $52\ \mu\text{m}$ and $7.31\ \mu\text{m}$, respectively, just very little and ignorable change compared with before hot-pressing the CH onto it. As the Al with a melt point of 660°C and an elasticity modulus of $70\ \text{Gpa}$, while the hot-press process with a temperature of 150°C , this temperature was not high enough to make Al soft and the pressure not large enough to make Al distort either. So the amplitude and

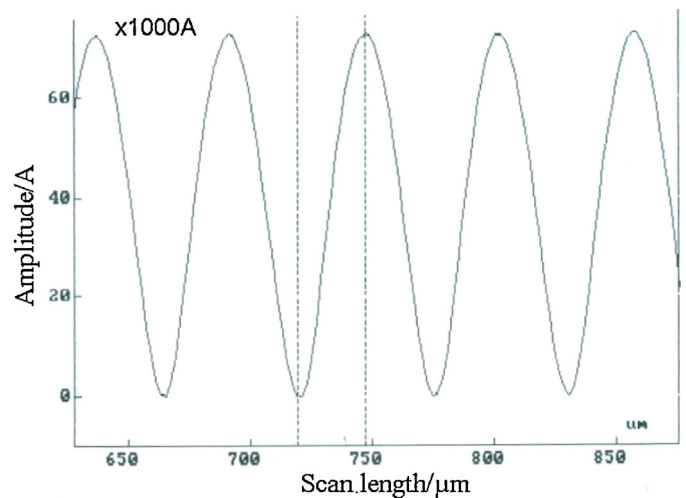


Fig. 10. Perturbation pattern on the surface of the Al foil after hot-press.

wavelength of the perturbation almost have no change after been hot-pressed.

4. Conclusions

A CH/Al dual-layer perturbation target was designed and fabricated for the hydrodynamic instability experiments in ICF. The target was composed of a perturbed Al foil and a CH layer. Uniform sinusoidal perturbation was introduced into the interface between the Al foil and the CH layer by SPDT technology. The CH layer was coated on the Al foil directly by a hot-press process. T , A , $H1$ and $H2$ of the CH/Al dual-layer perturbation target were $52\ \mu\text{m}$, $7.34\ \mu\text{m}$, $40\ \mu\text{m}$ and $15\ \mu\text{m}$, respectively. The cross-section images of the target showed that the CH layer coated on the perturbed Al foil perfectly. Surface roughness of the surface of CH layer was far less than the wavelength of the driven laser, the whole target meets the requirements of the hydrodynamic instability experiments well. As the process of coated the CH layer on the Al foil avoid the use of a sticker, eliminate the gaps between the CH layer and the Al foil, and almost have no influence to the amplitude and wavelength of the perturbation, it proved to be a simple and useful method for target fabrication and maybe much broader application in the future.

Acknowledgments

This work was supported by National Natural Science Foundation of China (51102184, 51172163), Shanghai Committee of Science and Technology (12nm0503001), National Science and Technology Support Program (SQ2011BAJY3505) and National High Technology Research and Development Program of China (2013AA031801).

References

- [1] S. Chandrasekhar, *Hydrodynamic and Hydromagnetic Stability*, Clarendon Press, Oxford, 1961.
- [2] R.D. Richtmyer, Taylor instability in shock acceleration of compressible fluids, *Commun. Pure Appl. Math.* 13 (1960) 297–319.
- [3] C.C. Kuranz, R.P. Drake, M.J. Grosskopf, A. Budde, C. Krauland, D.C. Marion, et al., Three-dimensional blast-wave-driven Rayleigh–Taylor instability and the effects of long-wavelength modes, *Phys. Plasmas* 16 (2009) 056310.
- [4] Y. Aglitskiy, A.L. Velikovich, M. Karasik, V. Serlin, C.J. Pawley, A.J. Schmitt, et al., Direct observation of mass oscillations due to ablative Richtmyer–Meshkov instability in plastic targets, *Phys. Rev. Lett.* 87 (2001) 265001.
- [5] R.L. McCrory, R.E. Bahra, R. Bettia, T.R. Boehly, T.J.B. Collins, R.S. Craxton, et al., OMEGA ICF experiments and preparation for direct drive ignition on NIF, *Nucl. Fusion* 41 (2001) 1413–1422.
- [6] C.J. Pawley, S.E. Bodner, J.P. Dahlburg, S.P. Obenshain, A.J. Schmitt, J.D. Sethian, et al., Observation of Rayleigh–Taylor growth to short wavelengths on Nike, *Phys. Plasmas* 6 (1999) 565–570.

- [7] M. Bono, D. Bennett, C. Castro, J. Satcher, J. Poco, B. Brown, et al., Fabrication of double shell targets with a glass inner capsule supported by SiO₂ aerogel for shots on the omega laser in 2006, *Fusion Sci. Technol.* 51 (2007) 611–625.
- [8] J.A. Marozas, F.J. Marshall, R.S. Craxton, I.V. Igumenshchev, S. Skupsky, M.J. Bonino, et al., Polar-direct-drive simulations and experiments, *Phys. Plasmas* 13 (2006) 056311.
- [9] C. Cherfils, S.G. Glendinning, D. Galmiche, B.A. Remington, A.L. Richard, S. Haan, et al., Convergent Rayleigh–Taylor experiments on the Nova laser, *Phys. Rev. Lett.* 83 (1999) 5507–5510.
- [10] B. Zhou, J. Wang, J. Shen, Z. Deng, Z. Lai, L. Chen, et al., Surface perturbation target for the Rayleigh–Taylor instability in inertial confinement fusion experiments, *J. Vac. Sci. Technol. A* 17 (1999) 3516–3520.
- [11] J. Kilkenny, K. Shillito, J. Kaae, H. Wilkens, D. Steinman, A. Greenwood, et al., Inertial confinement fusion targets. General Atomics Report, 2005, pp. 19–20.
- [12] K.O. Mikaelian, Design of a Rayleigh–Taylor experiment to measure strength at high pressures, *Phys. Plasmas* 17 (2010) 092701–092706.
- [13] X. Zhu, B. Zhou, A. Du, K. Chen, Y. Li, Z. Zhang, et al., Potential SiO₂/CRF bilayer perturbation aerogel target for ICF hydrodynamic instability experiment, *Fusion Eng. Des.* 87 (2012) 92–97.
- [14] N. Metzler, A.L. Velikovich, A.J. Schmitt, J.H. Gardner, Laser imprint reduction with a short shaping laser pulse incident upon a foam–plastic target, *Phys. Plasmas* 9 (2002) 5050–5058.
- [15] X. Zhu, B. Zhou, Y. Zhong, A. Du, K. Chen, Y. Li, et al., Design and fabrication of CH/CRF dual-layer perturbation target for ICF hydrodynamic experiment, *Nucl. Fusion* 51 (2011) 083044.
- [16] Y. Zhong, B. Zhou, J. Gui, A. Du, Z. Zhang, J. Shen, Fabrication of multilayer graded density peeled–carbon–aerogel target, *Fusion Eng. Des.* 86 (2011) 238–243.
- [17] H.C. Pant, M. Shukla, H.D. Pandey, Y. Kashyap, P.S. Sarkar, A. Sinha, et al., Enhancement of laser induced shock pressure in multilayer solid targets, *Laser Particle Beams* 24 (2006) 169–174.
- [18] X. Zhu, B. Zhou, X. Xu, Y. Zhong, A. Du, Y. Li, et al., Fabrication of multi-layered shock wave tube for hydrodynamic instability experiment, *J. Fusion Energy* 30 (2011) 509–515.
- [19] M. Shukla, Y. Kashyap, P.S. Sarkar, A. Sinha, H.C. Pant, R.S. Rao, et al., Laser induced shock pressure multiplication in multi layer thin foil targets, *Nucl. Fusion* 46 (2006) 419–431.
- [20] A.K. Knight, F.Y. Tsai, M.J. Bonino, D.R. Harding, Suitability of different polyimide capsule materials for use as ICF targets, *Fusion Sci. Technol.* 45 (2004) 187–196.
- [21] G.A. Kyrala, M.M. Balkey, C.W. Barnes, S.H. Batha, C.R. Christensen, J.A. Cobble, et al., Target fabrication: a view from the users, *Fusion Sci. Technol.* 45 (2004) 286–295.
- [22] E.J. Hsieh, C.W. Hatcher, D.E. Miller, Fabrication of Rayleigh Taylor instability experiment targets, *J. Vac. Sci. Technol. A* 3 (1985) 1278–1279.